Anisotropic rheology of a cubic medium and implications for geological materials

Laurent Pouilloux, Edouard Kaminski and Stéphane Labrosse

Équipe de Dynamique des Systèmes Géologiques - IPG Paris, Université Paris Diderot and CNRS,

4 place Jussieu, 75252 Paris cédex 05, France

SUMMARY

Dislocation creep, which is the dominant deformation mechanism in the upper mantle, results in a non-Newtonian anisotropic rheology. The implication of non-Newtonian rheology has been quite extensively studied in geodynamic models but the anisotropic aspect remains poorly investigated. In this paper we propose to fill this gap by (1) introducing a simple mathematical description of anisotropic viscosity and (2) illustrating the link between plastic crystal deformation and bulk material rheology. The study relies on the highest symmetry of the anisotropic tensor, a cubic symmetry, for which anisotropy is characterized by one parameter only, δ. First order implications of anisotropy are quantitatively explored as a function of δ. The effective rheology of the material is described as a function of the orientation of the crystals and of the imposed stress and the validity of the isotropic approximation is discussed. The model, applied to ringwoodite, a cubic crystal with spinel-type structure, predicts that the dynamics of the transition zone in the Earth's mantle is going to be strongly affected by mechanical anisotropy.

Key words: Dislocation creep – anisotropic rheology – geophysical materials – mantle convection.

1   INTRODUCTION

Modeling of solid state convection in the Earth mantle relies on a continuous medium description of the material properties. In the lower mantle, deformation is accommodated by diffusion creep which results in a Newtonian rheology. Classically, a Newtonian rheology has been used to model convection in the upper mantle as well. The influence of various parameters on the viscosity, such as temperature or grain size has been fully studied (e.g. Davaille & Jaupart 1994; Hall & Parmentier 2003). However, geodynamic models based on Newtonian rheology have not been able to self-consistently generate a plate like convective regime. Plate tectonics requires indeed a specific rheology that localizes deformation (Bercovici 2003), such as for example pseudo-plastic yielding (e.g. Tackley 2000) or a damage rheology (Bercovici & Ricard 2005). The question of the generation of plate tectonics thus boils down to the characterization of the effective rheology of the upper mantle.

Deformation in the upper mantle is mainly accommodated by dislocation creep which corresponds to a stress-dependent non-Newtonian rheology. Furthermore, as deformation at the crystal scale occurs on specific glide planes and along specific directions, it depends on the orientation of the crystal, which corresponds to an anisotropic rheology. The implications of stress dependent viscosity have been quite fully investigated (e.g. Tackley 2000; Ogawa 2003). On the other hand, general consequences of anisotropic viscosity have not been explored yet. A few studies (Richter & Daly 1978; Saito & Abe 1984; Honda 1986) have focused on the implications of anisotropic rheology for a hexagonal medium and have shown that anisotropy changes the value of the critical parameters for the onset of convection. Christensen (1987) studied the effect of anisotropic viscosity on both finite amplitude convection and post glacial rebound. He concluded that these effects were small in both situations. However these conclusions were obtained for a two-dimensional medium which does not encompass all the potential effects of anisotropy which by definition are fully tri-dimensional. In a three dimensional modeling of post glacial rebound for a transversally isotropic upper mantle, Han & Wahr (1997) found indeed some influence of anisotropy on the rate of horizontal motion.

In this article, we introduce a complete but simple mathematical description of anisotropic

viscosity that goes beyond the restrictions of a two-dimensional formulation. We use a simple medium with cubic symmetry, in which anisotropy is a function of one parameter only. We quantitatively investigate the first order implications of anisotropy and study its relationship with the plastic deformation of the crystals.

2   MATHEMATICAL FRAMEWORK

Viscosity describes the internal resistance of a fluid to flow. In an isotropic Newtonian fluid, the relationship between the stress tensor σ and the strain rate tensor $\dot{\epsilon}$ is given by

$$\sigma_{ij} = 2\mu\dot{\epsilon}_{ij} + \left(K - \frac{2}{3}\mu\right)\delta_{ij}\dot{\epsilon}_{kk}, \tag{1}$$

where μ is the dynamic viscosity (that gives the resistance to shear) and K the bulk viscosity (that controls the rate of volume change). The relationship becomes more general for an anisotropic fluid and is given by

$$\sigma_{ij} = \eta_{ijkl}\dot{\epsilon}_{kl}, \tag{2}$$

where η_{ijkl} represents the 81 components of a fourth order viscosity tensor. Due to the symmetry of σ_{ij} and $\dot{\epsilon}_{kl}$, and to the conservation of energy, only 21 components pf η_{ijkl} are independent (Landau & Lifchitz 1986). These symmetry properties allow one to reformulate the constitutive equation (2) using a second order tensor in a 6D space (Mehrabadi & Cowin 1990; Helbig 1994),

$$\begin{pmatrix} \sigma_{11} \\ \sigma_{22} \\ \sigma_{33} \\ \sqrt{2}\sigma_{23} \\ \sqrt{2}\sigma_{13} \\ \sqrt{2}\sigma_{12} \end{pmatrix} = \begin{pmatrix} \eta_{1111} & \eta_{1122} & \eta_{1133} & \sqrt{2}\eta_{1123} & \sqrt{2}\eta_{1113} & \sqrt{2}\eta_{1112} \\ \eta_{1122} & \eta_{2222} & \eta_{2233} & \sqrt{2}\eta_{2223} & \sqrt{2}\eta_{2213} & \sqrt{2}\eta_{2212} \\ \eta_{1133} & \eta_{2233} & \eta_{3333} & \sqrt{2}\eta_{3323} & \sqrt{2}\eta_{3313} & \sqrt{2}\eta_{3312} \\ \sqrt{2}\eta_{1123} & \sqrt{2}\eta_{2223} & \sqrt{2}\eta_{3323} & 2\eta_{2323} & 2\eta_{2313} & 2\eta_{2312} \\ \sqrt{2}\eta_{1113} & \sqrt{2}\eta_{2213} & \sqrt{2}\eta_{3313} & 2\eta_{2313} & 2\eta_{1313} & 2\eta_{1312} \\ \sqrt{2}\eta_{1112} & \sqrt{2}\eta_{2212} & \sqrt{2}\eta_{3312} & 2\eta_{2312} & 2\eta_{1312} & 2\eta_{1212} \end{pmatrix}\begin{pmatrix} \dot{\epsilon}_{11} \\ \dot{\epsilon}_{22} \\ \dot{\epsilon}_{33} \\ \sqrt{2}\dot{\epsilon}_{23} \\ \sqrt{2}\dot{\epsilon}_{13} \\ \sqrt{2}\dot{\epsilon}_{12} \end{pmatrix}, \tag{3}$$

or in compact notation,

$$\sigma_I = \eta_{IJ}\dot{\epsilon}_J, \tag{4}$$

with $I = i\delta_{ij} + (1-\delta_{ij})(9-i-j)$ and $J = k\delta_{kl} + (1-\delta_{kl})(9-k-l)$. This formulation is known as the Kelvin notation, which offers the advantage of having the same mathematical properties as the

initial fourth order tensor (hence the $\sqrt{2}$ factor). Due to additional crystallographic symmetries, the number of independent parameters η_{IJ} can be further reduced. An orthorhombic medium will be described by 9 independent components for example. In the following, we will focus on cubic symmetry because its anisotropy is defined by only one parameter and still illustrates the general consequences of an anisotropic rheology.

The tensor describing a given anisotropic medium η_{IJ} can be expressed as the sum of two contributions, an isotropic one η_{IJ}^{iso} and an anisotropic perturbation Δ_{IJ}^{aniso},

$$\eta_{IJ} = \eta_{IJ}^{iso} + \Delta_{IJ}^{aniso}. \tag{5}$$

The isotropic tensor writes as :

$$\eta^{iso} = \begin{pmatrix} \eta_{11} & \eta_{11} - \eta_{44} & \eta_{11} - \eta_{44} & 0 & 0 & 0 \\ \eta_{11} - \eta_{44} & \eta_{11} & \eta_{11} - \eta_{44} & 0 & 0 & 0 \\ \eta_{11} - \eta_{44} & \eta_{11} - \eta_{44} & \eta_{11} & 0 & 0 & 0 \\ 0 & 0 & 0 & \eta_{44} & 0 & 0 \\ 0 & 0 & 0 & 0 & \eta_{44} & 0 \\ 0 & 0 & 0 & 0 & 0 & \eta_{44} \end{pmatrix}. \tag{6}$$

This tensor has only two independent components, η_{11} and η_{44}, that can be related to the shear and bulk viscosities (defined in constitutive equation (1)), by using the expression of the eigenvalues of the tensor,

$$\lambda_1 = 3\eta_{11} - 2\eta_{44} = 3K, \tag{7}$$

$$\lambda_{2,3,4,5,6} = \eta_{44} = 2\mu, \tag{8}$$

which yields

$$\eta^{iso} = \begin{pmatrix} K + \frac{4}{3}\mu & K - \frac{2}{3}\mu & K - \frac{2}{3}\mu & 0 & 0 & 0 \\ K - \frac{2}{3}\mu & K + \frac{4}{3}\mu & K - \frac{2}{3}\mu & 0 & 0 & 0 \\ K - \frac{2}{3}\mu & K - \frac{2}{3}\mu & K + \frac{4}{3}\mu & 0 & 0 & 0 \\ 0 & 0 & 0 & 2\mu & 0 & 0 \\ 0 & 0 & 0 & 0 & 2\mu & 0 \\ 0 & 0 & 0 & 0 & 0 & 2\mu \end{pmatrix}. \tag{9}$$

A general cubic perturbation of this tensor will write as

$$
\Delta^{cubic} =
\begin{pmatrix}
\delta_1 & \delta_3 & \delta_3 & 0 & 0 & 0 \\
\delta_3 & \delta_1 & \delta_3 & 0 & 0 & 0 \\
\delta_3 & \delta_3 & \delta_1 & 0 & 0 & 0 \\
0 & 0 & 0 & \delta_2 & 0 & 0 \\
0 & 0 & 0 & 0 & \delta_2 & 0 \\
0 & 0 & 0 & 0 & 0 & \delta_2
\end{pmatrix},
\tag{10}
$$

where δ_1 is the perturbation of η_{11}, δ_2 is the perturbation of η_{44} and δ_3 is the perturbation of η_{12}. The three perturbation coefficients are linked by two physical constrains. First, the trace of the perturbation which is rotation-invariant represents its isotropic contribution and has to be zero, i.e. $\delta_1 = -\delta_2$. Second, the perturbed tensor has to keep the same resistance to isotropic compression as the isotropic reference tensor, i.e. the same ratio $\frac{\dot{\epsilon}_{ii}}{\sigma_{ii}}$, which yields

$$
3K + \delta_1 + 2\delta_3 = 3K,
\tag{11}
$$

or $\delta_1 = -2\delta_3$. The resulting cubic tensor can be expressed as a function of one anisotropy parameter only, $\delta = \eta_{11} - \eta_{44} - \eta_{12} = -5\delta_3$ (equal to 0 for an isotropic medium), and the two isotropic parameters, μ and K,

$$
\eta^{cubic} =
\begin{pmatrix}
K + \frac{4}{3}\mu + \frac{2}{5}\delta & K - \frac{2}{3}\mu - \frac{1}{5}\delta & K - \frac{2}{3}\mu - \frac{1}{5}\delta & 0 & 0 & 0 \\
K - \frac{2}{3}\mu - \frac{1}{5}\delta & K + \frac{4}{3}\mu + \frac{2}{5}\delta & K - \frac{2}{3}\mu - \frac{1}{5}\delta & 0 & 0 & 0 \\
K - \frac{2}{3}\mu - \frac{1}{5}\delta & K - \frac{2}{3}\mu - \frac{1}{5}\delta & K + \frac{4}{3}\mu + \frac{2}{5}\delta & 0 & 0 & 0 \\
0 & 0 & 0 & 2\mu - \frac{2}{5}\delta & 0 & 0 \\
0 & 0 & 0 & 0 & 2\mu - \frac{2}{5}\delta & 0 \\
0 & 0 & 0 & 0 & 0 & 2\mu - \frac{2}{5}\delta
\end{pmatrix}.
\tag{12}
$$

This expression is similar to the one obtained by Browaeys (2005) in the case of a cubic elastic tensor, based on the decomposition method (Browaeys & Chevrot 2004; Mehrabadi & Cowin 1990).

For a deviatoric stress tensor, the deformation is incompressible, and one can write, e.g. for σ_1,

$$
\sigma_1 = \left(K + \frac{4}{3}\mu + \frac{2}{5}\delta\right)\dot{\epsilon}_1 + \left(K - \frac{2}{3}\mu - \frac{1}{5}\delta\right)(\dot{\epsilon}_2 + \dot{\epsilon}_3),
\tag{13}
$$

$$= \left(2\mu + \frac{3}{5}\delta\right)\dot{\epsilon}_1,$$

using $\dot{\epsilon}_1 + \dot{\epsilon}_2 + \dot{\epsilon}_3 = 0$. Doing the same for σ_2 and σ_3, one obtains

$$\eta^{cubic} = \begin{pmatrix} 2\mu + \frac{3}{5}\delta & 0 & 0 & 0 & 0 & 0 \\ 0 & 2\mu + \frac{3}{5}\delta & 0 & 0 & 0 & 0 \\ 0 & 0 & 2\mu + \frac{3}{5}\delta & 0 & 0 & 0 \\ 0 & 0 & 0 & 2\mu - \frac{2}{5}\delta & 0 & 0 \\ 0 & 0 & 0 & 0 & 2\mu - \frac{2}{5}\delta & 0 \\ 0 & 0 & 0 & 0 & 0 & 2\mu - \frac{2}{5}\delta \end{pmatrix}, \tag{14}$$

where K is not a parameter anymore. The eigenvalues of the tensor are

$$\lambda_{1,2,3} = \frac{3}{5}\delta + 2\mu, \tag{15}$$

$$\lambda_{4,5,6} = -\frac{2}{5}\delta + 2\mu, \tag{16}$$

Because viscous dissipation is positive, these eigenvalues must be positive. This defines the stability domain for the tensor and the corresponding range of acceptable values for δ:

$$-\frac{10}{3} < \frac{\delta}{\mu} < 5. \tag{17}$$

We can now investigate the implications of anisotropic viscosity as a function of δ/μ.

3   IMPLICATIONS OF ANISOTROPIC VISCOSITY

3.1   Nominal anisotropy of a cubic medium

The value of the cubic perturbation δ can first be used to define a nominal percentage of anisotropy of the material, Δ. To do so, we use the ratio of the norm of the cubic perturbation tensor to the total tensor (isotropic contribution + cubic perturbation). The resulting expression for Δ depends only on δ/μ and is given by

$$\Delta = 100\frac{\|\eta_{IJ}^{total} - \eta_{IJ}^{iso}\|}{\|\eta_{IJ}^{total}\|} = 100\sqrt{\frac{(\delta/\mu)^2}{200 + 20(\delta/\mu) + 13(\delta/\mu)^2}}. \tag{18}$$

We show in figure 1 the percentage of anisotropy Δ as a function of δ/μ. The percentage of anisotropy depends on the sign of the perturbation, and as expected, is larger for larger values of $|\delta/\mu|$. By definition Δ cannot exceed 100%, and, because of the stability conditions given by
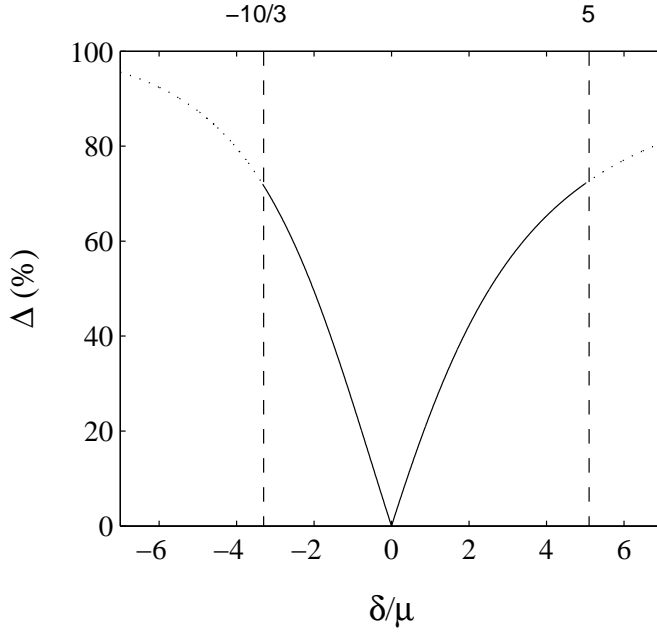
Figure 1. Percentage of anisotropy Δ as a function of the cubic perturbation δ/μ.

equation 17, is at most equal to 72% for $\delta/\mu=-10/3$ and $\delta/\mu=5$. These large numbers suggest that the anisotropic perturbation may have a significant effect on deformation, as illustrated below.

3.2 Degree of anisotropy and approximate isotropic rheology

In geodynamics, two major kinds of deformation are encountered. Viscosity estimates are made from post glacial rebound, which can be approximated by a pure shear, whereas simple shear is dominant in convective flows. Under the isotropic hypothesis, the same value of viscosity will be relevant for these two kinds of deformations. We evaluate the validity of this hypothesis as a function of the anisotropic perturbation δ/μ, by looking for the isotropic medium that best fits the actual deformation of the cubic medium. To do so, we minimize the error defined by:

$$\chi = 100\sqrt{\frac{(\dot{\epsilon}_I^{cubic} - \dot{\epsilon}_I^{iso})(\dot{\epsilon}_I^{cubic} - \dot{\epsilon}_I^{iso})}{\dot{\epsilon}_I^{cubic}\dot{\epsilon}_I^{cubic}}}, \tag{19}$$

where $\dot{\epsilon}_I^{cubic}$ is the actual strain rate tensor and $\dot{\epsilon}_I^{iso}$ is the strain rate tensor for the isotropic medium. The minimization of χ provides an "effective" shear viscosity μ_{eff} for the isotropic medium and an estimation of the error introduced by the isotropic approximation, χ_0.
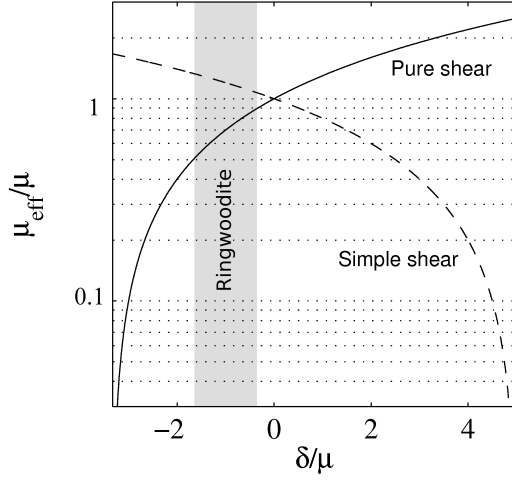
Figure 2. Effective dimensionless viscosity μ_{eff}/μ of the isotropic medium that best fits the deformation of the cubic material as a function of δ/μ. The solid and dashed lines correspond to pure shear and simple shear stress respectively. The gray region corresponds to the case of ringwoodite discussed in section 4.2.

If the stress principal directions are aligned with the crystallographic axes, the result can be analytically expressed as, for pure shear ($\sigma = (-1/2, -1/2, 1, 0, 0, 0)^T$),

$$\frac{\mu_{\mathrm{eff}}}{\mu} = \frac{3}{10}(\delta/\mu) + 1, \tag{20}$$

and for simple shear ($\sigma = (0, 0, 0, 0, 0, \sqrt{2})^T$),

$$\frac{\mu_{\mathrm{eff}}}{\mu} = -\frac{1}{5}(\delta/\mu) + 1. \tag{21}$$

We represent the value of the isotropic viscosity as a function of δ/μ in figure 2.

For pure shear, the best isotropic medium reproduces exactly the actual deformation ($\chi_0 = 0$ in equation 19). However, the effective viscosity of this isotropic medium is a function of δ/μ. For positive values of δ/μ the equivalent isotropic medium is only a bit stiffer than the reference isotropic medium that corresponds to $\delta/\mu = 0$. For negative values of δ/μ on the other hand, the medium becomes very soft. For $\delta/\mu = -3$ the effective viscosity is one order of magnitude softer than the reference isotropic medium. Close to the minimal value of δ/μ the medium becomes infinitely deformable (no resistance to stress). Note that this result does not imply that the viscosity tensor tends to the null tensor, but only that the coefficients of viscosity excited by the imposed stress (the three upper diagonal coefficients) tend to zero. At the maximum positive value of δ/μ

the three lower right diagonal coefficients tend also to zero, but they are not excited by the imposed stress and thus do not affect the effective viscosity.

For simple shear, the behavior of the cubic medium can also be exactly reproduced using the isotropic effective viscosity ($\chi_0 = 0$). For $\delta/\mu < 0$, the medium is a bit stiffer than the reference isotropic medium, whereas it can become very soft for $\delta/\mu > 0$. Here again, when δ/μ reaches the upper boundary of the stability domain, the medium presents no resistance to stress because the three lower right components of the tensor tend to 0. At the lower boundary of the stability domain, the three upper right components of viscosity also tend to 0 but are not excited by the imposed stress and thus do not affect the effective viscosity. When comparing the two viscosities predicted in figure 2, one notes that the consequences of anisotropy are opposite for the two deformations for positive (negative) δ/μ: the pure shear sees a stiffer (softer) medium whereas the shear stress sees a softer (stiffer) medium. A ratio of 10 and 0.1 between the two effective viscosities is found for $\delta/\mu = 3.91$ and $\delta/\mu = -2.81$, respectively. This suggests that using viscosity estimated from pure shear (e.g. post-glacial rebound) to model the deformation of the medium subject to a simple shear (e.g. convection) may introduce strong bias. We thus do not confirm the conclusion of Christensen (1987) that mechanical anisotropy has a second order effect only. This discrepancy is related to the difference between our 3D formalism and Christensen's 2D approach valid only for a layered medium. Our results are closer to the conclusion of Han & Wahr (1997) based also on a 3D modeling.

3.3   The effect of arbitrary orientations

The results become more complex than presented above if the principal axes of the stress tensor are not aligned with the crystallographic axes. To illustrate the influence of the orientation of the crystal, we consider a cubic medium vertically tilted by an angle θ and rotated by an angle ϕ in the horizontal plane. For the sake of the argument, we take a cubic medium with $\delta/\mu = 2$, i.e. an anisotropy of Δ=44%. From equation 19 we determine the isotropic viscosity that best fits the actual deformation (effective viscosity) and the associated error as a function of θ and ϕ, for simple shear. Results displayed in figure 3 show that the effective value of viscosity is not much
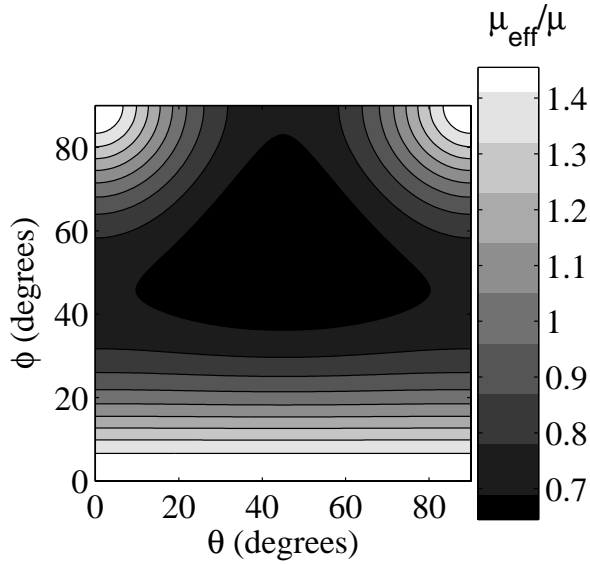
Figure 3. Isocontours of the ratio between the effective viscosity and the reference viscosity, as a function of θ and ϕ, for pure shear.
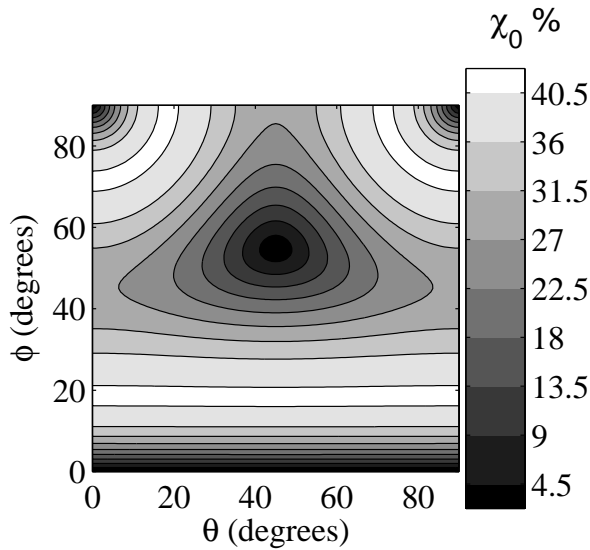

Figure 4. Isocontours of χ_0, the difference between the actual strain rate tensor and the one obtained for the best fitting isotropic medium, for pure shear.

affected by the orientation of the crystal (less than a factor 2), and is thus mainly controlled by the value of δ/μ. However, the errors introduced by the isotropic approximation, plotted on figure 4, show that there is usually no equivalent isotropic medium to a rotated cubic medium, except for specific orientations. The large errors come from the fact that, because of the coupling induced by the anisotropic viscosity coefficients, the principal axes of deformation are not aligned anymore
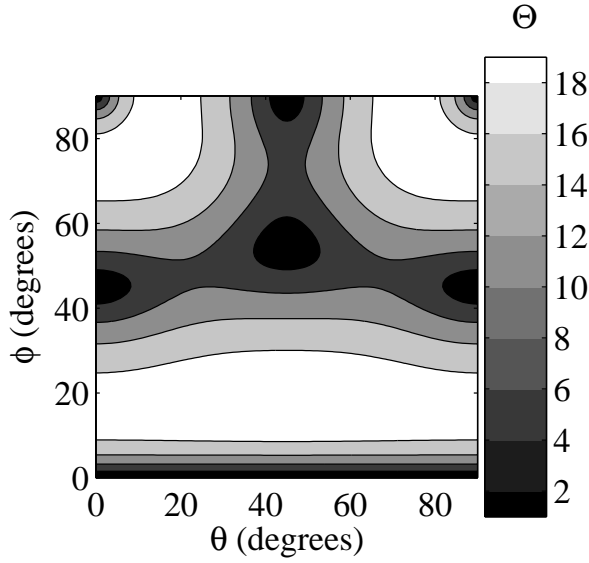
Figure 5. Angle in degree Θ between the direction of maximum extension rate and the z-direction, for pure shear.

with the principal axes of the stress tensor. To explore this point, we plot on figure 5 the angle between the vertical axis and the direction of maximal extension rate. As this angle is usually non zero, the directions of the principal axes of the strain ellipsoid cannot be used to infer directly the orientation of principal axes of the stress, for an anisotropic medium. The isotropic approximation thus generally introduces error both in the values of the strain rate and in the inferred directions of eigenvectors of the strain rate tensor.

We have described in this section the effects of anisotropic viscosity for theoretical mediums characterized by an arbitrary value of the cubic perturbation δ/μ. In the next section we show how the value of δ/μ can be related to the mechanical parameters of a cubic crystal.

4   FROM DISLOCATION CREEP TO ANISOTROPIC VISCOSITY TENSOR

4.1   Dislocation creep in cubic crystals

Plastic deformation in a crystal is a function of the activity and orientation of prescribed slip systems (e.g. Poirier 1985), and five independent active slip systems are required to accommodate an arbitrary deformation (Von Mises' criterion). To define a canonical cubic crystal that fulfills the Von Mises' criterion, we consider a FCC crystal with two families of slip planes characterized by

two different critical resolved shear stress (CRSS). The first family of slip systems corresponds to $(111)[\bar{1}10]$ with CRSS τ_0^1 (4 planes with 3 slip directions = 12 slip systems) and the second family corresponds to $(001)[\bar{1}10]$ with CRSS τ_0^2 (3 planes with 2 slip directions = 6 slip systems). The plastic deformation of the crystal is given by (e.g. Kaminski & Ribe 2001)

$$\dot{\epsilon}_{ij} = 2\dot{\epsilon}_0 \sum_{s=1}^{18} \left(\left| \frac{\sigma_{pq}l_p^s n_q^s}{\tau_0^s} \right|^{n-1} \frac{\sigma_{pq}l_p^s n_q^s}{\tau_0^s} \right) l_i^s n_j^s, \tag{22}$$

where $\mathbf{l^s}$ and $\mathbf{n^s}$ are unit vectors in the slip direction and normal to the slip plane of the slip system s, respectively. The stress exponent n is usually larger than 1 for dislocation creep, but we focus here on anisotropic effects and we will keep $n=1$ for the sake of the argument. Equation 22 can be rewritten as

$$\frac{\dot{\epsilon}_I}{\dot{\epsilon}_0} = S_{IJ}^* \frac{\sigma_J}{\tau_0^1}, \tag{23}$$

with S^*, the dimensionless compliance tensor, given by

$$S^* = \eta^{-1}\frac{\tau_0^1}{\dot{\epsilon}_0} = \frac{2}{3} \begin{pmatrix} 6 & 0 & 0 & 0 & 0 & 0 \\ 0 & 6 & 0 & 0 & 0 & 0 \\ 0 & 0 & 6 & 0 & 0 & 0 \\ 0 & 0 & 0 & \frac{3+2\tau^*}{\tau^*} & 0 & 0 \\ 0 & 0 & 0 & 0 & \frac{3+2\tau^*}{\tau^*} & 0 \\ 0 & 0 & 0 & 0 & 0 & \frac{3+2\tau^*}{\tau^*} \end{pmatrix}, \tag{24}$$

with $\tau^* = \frac{\tau_0^2}{\tau_0^1}$. The expressions of the isotropic viscosity and of the cubic perturbation parameter δ/μ are found by comparison with equation 14:

$$\mu = \frac{3 + 11\tau^*}{20(3 + 2\tau^*)}\frac{\tau_0^1}{\dot{\epsilon}_0}, \tag{25}$$

$$\frac{\delta}{\mu} = \frac{5(-4\tau^* + 3)}{3 + 11\tau^*}. \tag{26}$$

The value of δ/μ as a function of τ^* is shown in figure 6, where one can see that the limit of stability is reached when $\tau^* \to 0$ ($\delta/\mu = 5$) whereas an isotropic behavior is found for τ^*=3/4. The minimal value is $\delta/\mu = -20/11$ which falls within the stability domain.

Some geological materials present a cubic symmetry and can be mechanically described using a FCC model, for example halite and spinel-type ringwoodite. The first material is relevant for
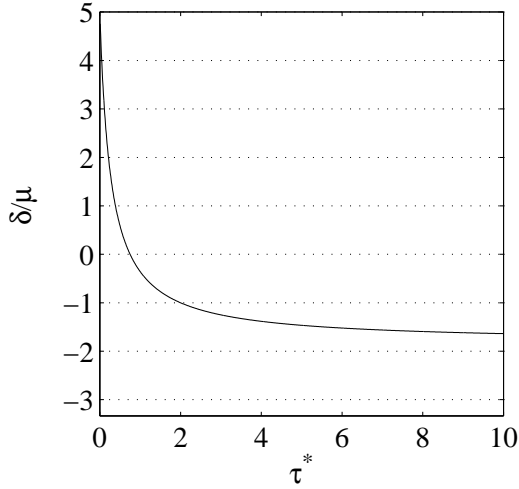
Figure 6. Value of the cubic perturbation δ/μ as a function of the ratio of the critical resolved shear stresses τ^* in a FCC crystal.

the dynamics of salt diapirs whereas the second one is relevant for the dynamics of the transition zone. In these two minerals, the $(111)[\bar{1}10]$ family of slip systems is softer than the second family $(001)[\bar{1}10]$ at room conditions and under high pressure (10 GPa), which yields a value of τ^* between 2 and 10 (Lebensohn et al. 2003; Wenk et al. 2005; Carrez et al. 2006), or δ/μ between -1 and -1.64. At the high temperature and pressure conditions of the transition zone (1800 K, 20 GPa), potential slip systems will tend to have similar critical resolved shear stress (Wenk et al. 2005), and a value of τ^*=1 can be used as a lower bound, or $\delta/\mu = -0.35$, which yields a total range of $-1.64 \leq \delta/\mu \leq -0.35$. The results from the preceding section show that the values of δ/μ for geologically relevant crystals fall in a range in which anisotropy has some major effects (see Figure 2). First the effective viscosity is going to be a function of the geometry of the imposed stress and second if the crystals are not perfectly aligned with the principal direction of stress, an additional rotation of the strain ellipsoid will be induced by anisotropic coupling.

4.2 The case of a ringwoodite polycrystal : implications of the lattice preferred orientation

The previous conclusions were obtained for a single crystal and we illustrate here how they change for a polycrystal. The anisotropic viscosity of a polycrystalline aggregate is a function both the anisotrotropic tensor of the single crystal and the distribution of orientation of the crystals. There is different ways of averaging crystal properties in an aggregate, the two end-members being the
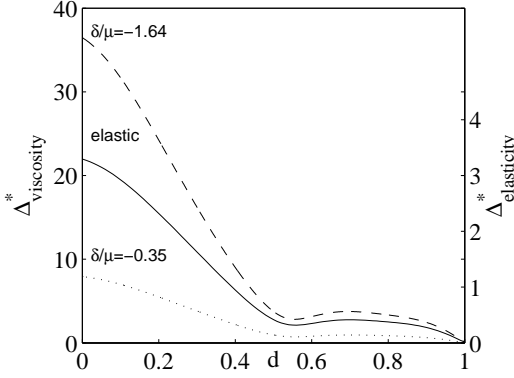
Figure 7. Anisotropy parameter Δ^* for ringwoodite polycrystal for extremal values of δ/μ, as a function of dispersion (left y-axis). We also present for reference the elastic anisotropy as a function of disperions (solid line, right y-axis).

Voigt average (homogeneous strain rate) and the Reuss average (homogeneous stress). The Voigt average is defined by

$$\eta_{Voigt} = \frac{1}{N} \sum_{\nu=1}^{N} \eta_{ij}^{\nu}, \tag{27}$$

where N the number of crystals and η_{ij}^{ν} the viscosity tensor for crystal ν, depending on the orientation of the crystal ; the Reuss average is defined by

$$\eta_{Reuss}^{-1} = \frac{1}{N} \sum_{\nu=1}^{N} \left(\eta_{ij}^{\nu} \right)^{-1}. \tag{28}$$

For a uniform distribution of crystal orientation, the polycrystal will be equivalent to an isotropic medium. Using a Voigt average, the cubic perturbation will cancel out and the resulting viscosity will be the isotropic part of the single crystal viscosity tensor. As the Reuss average is based on compliance instead of viscosity, the cubic perturbation will not cancel out and the isotropic viscosity will depend on δ/μ. Only the Voigt average is thus fully consistent with our formalism, whereas the Reuss average would require to define a compliance perturbation instead of a viscosity perturbation. A detailed discussion of the averaging procedure is beyond the scope of this article but, nevertheless, we checked that its influence on the results presented below is small.

We use a lattice preferred orientation (LPO) uniformly distributed on a domain ($\phi_1 = [0, d\pi]$, $\cos(\theta) = [1 - 2d, 1]$,$\phi_2 = [0, d\pi]$) where ϕ_1, θ, ϕ_2 are Euler angles and d is a dispersion parameter between 0 and 1. For $d = 1$, the distribution is uniform over the whole Eulerian space and the medium is isotropic. For $d \to 0$, the distribution becomes sharper and the polycrystal becomes

equivalent to a single crystal. The reference isotropic tensor is thus now defined by $d = 1$. As in section 2 we introduce an anisotropy parameter to quantify the difference between the actual polycrystal tensor and the isotropic polycrystal tensor ($d = 1$),

$$\Delta^* = 100 \frac{\|\eta_{IJ} - \eta_{IJ}^{d=1}\|}{\|\eta_{IJ}\|}. \tag{29}$$

This parameter is shown on figure 7 for the two extreme values of δ/μ for ringwoodite. For $d \to 1$, $\Delta^* \to 0$ as the medium becomes isotropic, whereas for $d \to 0$, $\Delta^* \to \Delta$ corresponding to the monocrystal. We can see that a low seismic anisotropy (2%) corresponds to a sharp LPO and will produce a significant anisotropic mechanical behavior. In the following, we explore this effect for three stress conditions and for various LPO dispersion parameter d.

We apply a simple shear, a pure shear and a combined stress $\sigma = (1, -1, 0, 0, 0, \sqrt{2})^T$ on the polycrystal, using $\delta/\mu = -1.64$ and $\delta/\mu = -0.35$. For each case, we determine both the effective viscosity μ_{eff} and the associated error χ_0 corresponding to the best fitting isotropic medium. Two main results are shown on figure 8. First, the effective viscosity of the polycrystal depends weakly on d, which means that the aggregate viscosity is primarily a function of the monocrystal anisotropy. Second, the isotropic approximation introduces significant errors for $d < 0.5$ and is not valid, especially for $\delta/\mu = -1.64$. These errors are complex functions of d because the medium does not display any particular symmetry for $d \neq 0$ and $d \neq 1$. In general there is no isotropic medium that matches exactly the deformation and the effective viscosity depends weakly on the stress configuration.

The previous results bear some implications for the mechanical properties of the transition zone. These properties are going to be a function of δ/μ for ringwoodite as discussed above and of lattice preferred orientation (d). Seismic anisotropy in the transition zone is weak but maybe as large as 2% (Trampert & van Heijst 2002). This value can be used to estimate the value of d from the elastic tensor of the monocrystal. As the elastic anisotropy of a ringwoodite monocrystal is also small (about 3% Karki et al. 2001), it implies quite a sharp LPO of ringwoodite in the transition zone (see figure 7). We can thus conclude that the rheology of the transition zone is significantly anisotropic. As a consequence a slab going through and a plume spreading under the transition zone will not see the same effective medium. Furthermore, seismic anisotropy is
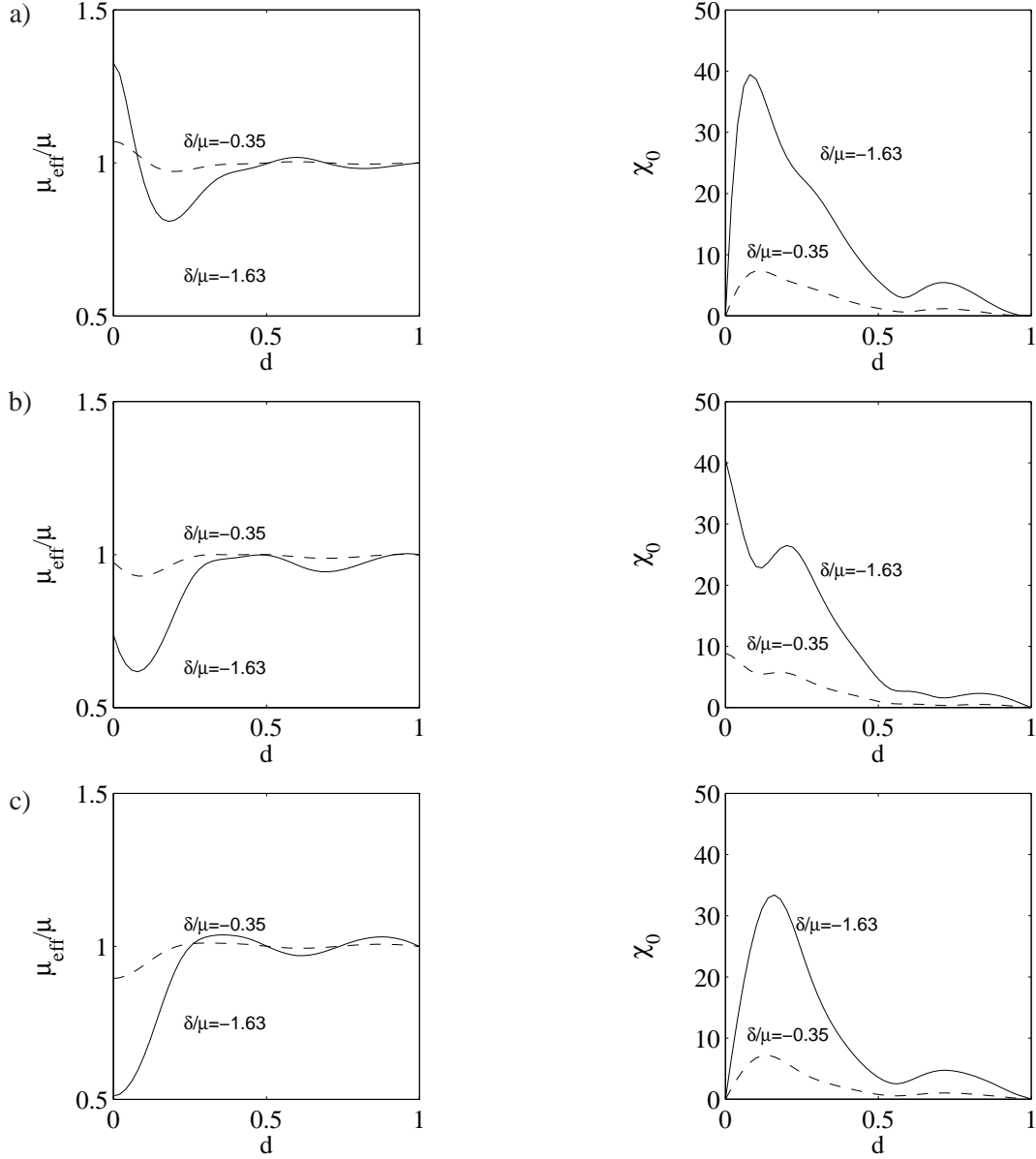
Figure 8. Effect of lattice preferred orientation on effective viscosity. a) Value of the effective viscosity μ_{eff}/μ and of the error χ_0, for simple shear as a function of the LPO dispersion d. b) Same for a combined stress defined by $\sigma = (1, -1, 0, 0, 0, \sqrt{2})^T$. c) Same for a pure shear. The solid line corresponds to $\delta/\mu = -1.64$ and the dashed line to $\delta/\mu = -0.35$.

laterally heterogeneous in the transition zone which implies also mechanical heterogeneities that may affect the strength and geometry of the convective flow through the transition zone.

5   CONCLUSION

The description of anisotropic viscosity using a fourth-order tensor can be simply formalised based on tensor perturbation in a 6 dimensional space. This technique applied to the cubic symmetry allows a straightforward exploration of the range of effects of cubic anisotropic viscosity. Unlike in the previous study of Christensen (1987) based on a layered medium, we found here that mechanical anisotropy is potentially important. The main effect is that the effective viscosity for a given medium does depend on the geometry of the applied stress and that there is no unique isotropic medium that can reproduce the complex behaviour of an anisotropic medium.

Misalignment between the principal axes of the viscosity tensor and that of the applied stress also modifies the effective viscosity compared to the aligned case and, additionnally, gives the strain rate tensor axes still another direction. In this situation, the actual strain rate cannot be obtained by any equivalent isotropic medium.

The viscosity estimated for a given geodynamical process, like post-glacial rebound, may not be valid for another, like convection, even without mentioning others complexities like timescale- or temperature-dependent viscosity (e.g. Čadek & Fleitout 2003).

Cubic symmetry is the highest anisotropic symmetry and probably represents a lower bound of the range of effect of mechanical anisotropy. The method we have presented can be used to investigate the anisotropy of more complex crystals. Their description can however become tedious beyond the hexagonal symmetry which is still tractable (three independent anisotropy parameters instead of one here). Furthermore, natural polycrystals will not always be described by simple viscosity symmetry and will result in a more complex behaviour, including potential feedback between LPO development and effective viscosity (Muhlhaus et al. 2004). The case of ringwoodite in the transition zone explored above provides an example of the richness of real systems. Deciphering these effects in geodynamical observations like post-glacial rebounds or small-scale convection is challenging and the link between seismic and mechanical anisotropy mainly remains to be explored (e.g. Moresi & Muhlhaus 2006). However, our formalism is simple enough to be straightforwardly included in numerical codes used to model convection in planetary mantles. The development of LPO in mantle flow makes the effective viscosity sensitive to the type and orienta-

tion of stress. This mechanism might contribute to the weakening necessary for mantle convection to evolve in a plate tectonics regime.

REFERENCES

Bercovici, D., 2003, The generation of plate tectonics from mantle convection, *Earth Planet. Sci. Lett.*, **205**, 107–121.

Bercovici, D. & Ricard, Y., 2005, Tectonic plate generation and two-phase damage: Void growth versus grain size reduction, *J. Geophys. Res.*, **110**, 3401–3419.

Browaeys, J. T., 2005, *Modélisation directe de l'anisotropie sismique mantellique en contexte de point chaud : Hawaii et Islande*, Ph.D. thesis, Institut de Physique du Globe de Paris.

Browaeys, J. T. & Chevrot, S., 2004, Decomposition of the elastic tensor and geophysical applications, *Geophys. J. Int.*, **159**, 667–678.

Carrez, P., Cordier, P., Mainprice, D., & Tommasi, A., 2006, Slip systems and plastic shear and anisotropy in Mg_2SiO_4 ringwoodite: insights from numerical modelling, *Eur. J. Mineral.*, **18**, 149–160.

Christensen, U. R., 1987, Some geodynamical effects of anisotropic viscosity, *Geophys. J. R. Astr. Soc.*, **91**, 711–736.

Davaille, A. & Jaupart, C., 1994, Onset of thermal convection in fluids with temperature-dependent viscosity: Application to the oceanic mantle, *J. Geophys. Res.*, **99**, 19853–19866.

Hall, C. E. & Parmentier, E. M., 2003, Influence of grain size evolution on convective instability, *Geochem. Geophys. Geosyst.*, **4**, doi:10.1029/2002GC000308.

Han, D. & Wahr, J., 1997, An analysis of anisotropic mantle viscosity, and its possible effects on postglacial rebound, *Phys. Earth Planet. Inter.*, **102**, 33–50.

Helbig, K., 1994, Representation and approximation of elastic tensors, Poster P1-1 at the 6th International Workshop on Seismic Anisotropy (Trondheim).

Honda, S., 1986, Strong anisotropic flow in a finally layered asthenosphere, *Geophys. Res. Lett.*, **13**, 1454–1457.

Kaminski, E. & Ribe, N. M., 2001, A kinematic model for recrystallisation and texture development in olivine polycrystals, *Earth Planet. Sci. Lett.*, **289**, 253–267.

Karki, B. B., Stixrude, L., & Wentzcovitch, R., 2001, High pressure elastic properties of major materials of Earth's mantle from first principle, *Geophys. Res. Lett.*, **39**, 507–534.

Landau, L. & Lifchitz, E., 1986, *Theory of elasticity*, Butterworth Heineman, Oxford.

Lebensohn, R. A., Dawson, P. R., Kern, H. M., & Wenk, H.-R., 2003, Heterogeneous deformation and texture development in halite polycrystals: comparison of different modeling approaches and experimental data, *Tectonophysics*, **379**, 287–311.

Mehrabadi, M. M. & Cowin, S. C., 1990, Eigentensors of linear anisotropic elastic materials, *Q. Jl Mech. appl. Math.*, **43**, 15–41.

Moresi, L. & Muhlhaus, H.-B., 2006, Anisotropic viscous models of large-deformation mohrcoulomb failure, *Philosophical Magazine*, **86**, 3287–3305.

Muhlhaus, H.-B., Moresi, L., & Cada, M., 2004, Emergent anisotropy and flow alignment in viscous rock, *Pure appl. geophys.*, **161**, 2451–2463.

Ogawa, M., 2003, Plate-like regime of a numerically modeled thermal convection in a fluid with temperature-, pressure-, and stress-history-dependent viscosity, *J. Geophys. Res.*, **108**, 2–18, doi:10.1029/2000JB000069.

Poirier, J.-P., 1985, *Creep of crystals*, Cambridge University Press, Cambridge.

Richter, F. M. & Daly, S., 1978, Convection models having a multiplicity of large horizontal scales, *J. Geophys. Res.*, **83**, 4951–4956.

Saito, M. & Abe, Y., 1984, Consequences of anisotropic viscosity in the Earth's mantle, *Jishin*, **37**, 237–245, In Japanese with english abstract and figure captions.

Tackley, P. J., 2000, Mantle convection and plate tectonics: Toward an integrated physical and chemical theory, *Science*, **288**, 2002–2007.

Trampert, J. & van Heijst, H. J., 2002, Global azimuthal anisotropy in the transition zone, *Science*, **296**, 1297–1299.

Čadek, O. & Fleitout, L., 2003, Effect of lateral viscosity variations in the top 300 km on the geoid and dynamic topography, *Geophys. J. Int.*, **152**, 566–580.

Wenk, H.-R., Ischia, G., Nishiyama, N., Wang, Y., & Uchida, T., 2005, Texture development and deformation mechanisms in ringwoodite, *Phys. Earth Planet. Inter.*, **152**, 191–199.